

# Polymer-Solvent Diffusion and Equilibrium Parameters by Inverse Gas-Liquid Chromatography

Ilyess Hadj Romdhane and Ronald P. Danner

Dept. of Chemical Engineering, The Pennsylvania State University, University Park, PA 16802

*The solubility and diffusion coefficients of low-molecular-weight penetrants in a polymeric stationary phase were determined by use of inverse gas chromatography (IGC). Previously reported applications of packed-column IGC to the measurement of the stationary-phase diffusion coefficient have been carried out via the van Deemter approach. We present here a new mathematical model to describe the chromatographic process in packed columns. A moment analysis procedure was developed from this model to analyze the chromatographic peaks eluting from packed columns. The first moment (mean retention time) is determined to depend only on the equilibrium partition coefficient, whereas the second moment (variance) is related to both the thermodynamic and transport properties of the polymer-solute system. The validity of the technique was demonstrated by measuring the diffusivity and solubility of toluene and benzene in polystyrene above the glass transition temperature of the polymer. Free-volume theory was used to interpret and correlate the diffusivity data obtained at infinite dilution of the solute. One can use the results obtained at infinite dilution to predict reliably via the free-volume theory the concentration and temperature dependence of polymer-solvent diffusion coefficients.*

## Introduction

Conventional methods for measuring diffusion coefficients rely on bulk equilibration and gravimetric vapor sorption/desorption experiments. These methods, however, become very difficult to apply to polymer-solvent systems when the solvent is present in vanishingly small amounts. The low diffusivity value, characteristic of polymer-solvent systems, is at the origin of the experimental difficulties encountered with classical techniques. As a consequence, only a small amount of diffusivity data for polymer solutions in the highly polymer concentrated region is available in the literature. This region, however, is of primary interest in the polymer industry, particularly in the manufacture of polymer films, which often must be free of volatile matter for environmental and safety reasons.

In recent years, attention has been focused on the use of inverse gas chromatography as an alternative method for studying transport properties in concentrated polymer solutions. Most of the previous work (Gray and Guillet, 1973;

Kong and Hawkes, 1976; Tait and Abushihada, 1979; Hu et al., 1987) was done using packed chromatographic columns with data analysis in terms of the van Deemter equation (van Deemter et al., 1956). Moment analysis models for the chromatographic process in capillary columns were also developed and used effectively to measure diffusion coefficients in polymer-solvent systems (Pawlich et al., 1987, 1988; Arnould and Laurence, 1989). In this work, we present a formulation of a new mathematical model (packed-column inverse gas chromatography model, PCIGC) to describe the elution process in packed columns and to evaluate the moment analysis method for determining the partition and diffusion coefficients. The applicability of the model is discussed in light of recent experimental results obtained by packed-column inverse gas chromatography.

## Model of the Chromatographic Process

In this study, the system consists of a cylindrical packed column filled with support particles (Chromosorb W-HP, 80-

Correspondence concerning this article should be addressed to R. P. Danner.

100 mesh) coated with a polymer substrate. The coating thickness,  $d_p$ , is assumed to be uniform. The fractional volume of the mobile phase (carrier gas) is  $\epsilon_g$  and the fractional volume of the stationary phase (polymer substrate) is  $\epsilon_p$ . The diffusion coefficient of the solute in the carrier gas and the polymer phase are  $D_L$  and  $D_p$ , respectively. The length of the column is  $L$ ; the carrier gas moves with an average linear velocity  $v$ . The expansion of the carrier gas, due to pressure gradients across the packed column, is taken into account in the moment analysis method, discussed later. The thermodynamic equilibrium between the gas phase and the polymer layer at the surface is assumed to be instantaneous. Surrounding the coated particle is a gas film characterized by an external fluid-film mass-transfer coefficient,  $k_f$ . The analysis and modeling of the system consist of finding a mathematical representation of the physicochemical processes tying output and input variables together. To formulate this model, the following assumptions are made:

- The system is isothermal.
- The particles are assumed to be spherical in shape.
- The polymer film is constant in thickness.
- Axial diffusion in the stationary phase is negligible.
- The carrier gas is insoluble in the polymer.
- The absorption isotherm is linear.
- No surface adsorption occurs at the polymer-gas interface.
- No chemical reaction occurs between the solute and the polymer.
- Diffusion coefficients are concentration-independent.
- The effects of mixing in the injection and detector chambers are negligible.
- The injected sample enters the column as a narrow pulse so that the inlet concentration can be modeled as an impulse function.

## Theory

The partial differential equation governing the transport of the solute within the polymer phase in spherical coordinates is written as follows:

$$\frac{\partial q}{\partial t} = \frac{D_p}{r^2} \frac{\partial}{\partial r} \left( r^2 \frac{\partial q}{\partial r} \right) \quad (1)$$

where  $q(r, z, t)$  is the concentration of the solute in the polymer phase as a function of radial direction  $r$ , axial direction  $z$ , and time,  $t$ . Equation 1 is subject to the following initial and boundary conditions:

$$q(r, z, t=0) = 0 \quad (2)$$

At the support surface, there is no solute flux inside the particle:

$$\left[ \frac{\partial q}{\partial r} \right]_{r=R_s} = 0 \quad (3)$$

and at the polymer-gas interface, we have:

$$D_p \left[ \frac{\partial q}{\partial r} \right]_{r=R_p} = k_f \left\{ C(z, t) - \frac{[q(r, z, t)]_{r=R_p}}{K} \right\} \quad (4)$$

where  $C(z, t)$  is the bulk solute concentration in the mobile phase as a function of axial direction,  $z$ , and time,  $t$ ;  $K$  is the equilibrium partition coefficient, and  $R_s$  and  $R_p$  are the radius of the support particle and the polymer film, respectively. The partial differential equation, Eq. 1, subject to the initial and boundary conditions, Eqs. 2, 3 and 4, may be solved in the Laplace domain to yield the solute concentration in the polymer phase as a function of  $r$ ,  $z$ , and  $C(z, t)$ . The solution is:

$$\bar{q}(r, z, s) = \frac{k_f R_p^2}{r D_p} \bar{C}(z, s) \left[ \frac{\sinh(\alpha r) + A(\alpha) \cosh(\alpha r)}{\left( A(\alpha) \alpha R_p - 1 + \frac{k_f R_p}{K D_p} \right) \sinh(\alpha R_p) + \left( \alpha R_p - A(\alpha) + A(\alpha) \frac{k_f R_p}{K D_p} \right) \cosh(\alpha R_p)} \right] \quad (5)$$

where

$$\alpha = \left( \frac{s}{D_p} \right)^{1/2} \quad (6)$$

and

$$A(\alpha) = - \left[ \frac{\sinh(\alpha R_s) - \alpha R_s \cosh(\alpha R_s)}{\cosh(\alpha R_s) - \alpha R_s \sinh(\alpha R_s)} \right] \quad (7)$$

In Eq. 5,  $\bar{q}(r, z, s)$  and  $\bar{C}(z, s)$  are the Laplace transforms of  $q(r, z, t)$  and  $C(z, t)$ , respectively. The volume-average concentration of the solute in the polymer phase may then be obtained as follows:

$$Q(z, t) = \frac{\int_{R_s}^{R_p} 4\pi r^2 q(r, z, t) dr}{\int_{R_s}^{R_p} 4\pi r^2 dr} \quad (8)$$

or

$$Q(z, t) = \frac{3}{(R_p^3 - R_s^3)} \int_{R_s}^{R_p} r^2 q(r, z, t) dr \quad (9)$$

Integration of Eq. 9, using Eq. 5, in the Laplace domain yields:

$$\bar{Q}(z, s) = \left[ \frac{\Phi(s)}{\Phi(s) \frac{\alpha^2 (R_p^3 - R_s^3) D_p}{3 k_f R_p^2} + 1} \right] \bar{C}(z, s) \quad (10)$$

where  $\bar{Q}(z, s)$  is the Laplace transform of  $Q(z, t)$ , and

$$\Phi(s) = \frac{3KR_p}{\alpha^2(R_p^3 - R_s^3)} \left\{ \frac{(\alpha R_s)^2 + \alpha^2 R_s d_f - 1 + \alpha d_f \coth(\alpha d_f)}{\alpha R_s \coth(\alpha d_f) + 1} \right\} \quad (11)$$

where  $d_f$  is the polymer film thickness.

To relate the thermodynamic and diffusion parameters to the chromatographic data obtained from the detector output, one should solve for the solute concentration in the gas phase,  $C(z, t)$ . An overall material balance around the packed chromatographic column gives the following partial differential equation:

$$\frac{\partial C}{\partial t} + \frac{\epsilon_p}{\epsilon_g} \frac{\partial Q}{\partial t} + v \frac{\partial C}{\partial z} - D_L \frac{\partial^2 C}{\partial z^2} = 0 \quad (12)$$

The initial and boundary conditions are:

$$C(z, t=0) = Q(z, t=0) = 0 \quad (13)$$

also,

$$C(z=0, t) = \delta(t) C_o \quad (14)$$

and

$$\lim_{z \rightarrow \infty} C(z, t) = 0 \quad (15)$$

where  $\delta(t)$  is the Dirac delta function, and  $C_o$  is the strength of the inlet impulse. Using the expression for  $\bar{Q}$ , Eq. 10, the solution of Eqs. 12-15 in the Laplace domain is:

$$\bar{C}(z, s) = C_o \exp$$

$$\left[ \left( \frac{v}{2D_L} - \sqrt{\left( \frac{v}{2D_L} \right)^2 + \frac{s}{D_L} \left( 1 + \frac{\epsilon_p}{\epsilon_g} \Psi(s) \right)} \right) z \right] \quad (16)$$

where

$$\Psi(s) = \frac{\Phi(s)}{\Phi(s) \frac{\alpha^2(R_p^3 - R_s^3)D_p}{3k_f R_p^2} + 1} \quad (17)$$

and  $\Phi(s)$  is given by Eq. 11. At the exit of the column, where  $z = L$ , the solution can be written as:

$$\bar{C}(L, s) = C_o \exp \left[ \frac{Pe}{2} - \sqrt{\frac{Pe^2}{4} + \frac{sL^2}{D_L} \left( 1 + \frac{\epsilon_p}{\epsilon_g} \Psi(s) \right)} \right] \quad (18)$$

where  $Pe$  is the Peclet number defined as:

$$Pe = \frac{vL}{D_L} \quad (19)$$

Here,  $v$  and  $D_L$  are the average values of the velocity of the

carrier gas and the longitudinal diffusion coefficient, respectively. The inclusion of the effect of pressure variation across the column on these two parameters is a major source of complexity in the resulting differential equation. We chose instead to use average values which could easily be related to the measured values at the exit of the column. This is usually done by incorporating pressure correction terms, discussed later, to take into account the expansion of the carrier gas along the column.

### Moment analysis

While the transform expression, Eq. 18, is difficult to invert analytically, its numerical inversion is simple and more convenient. In this study, the theoretical profiles are simulated by numerical inversion of the transform equation by employing a program using a Fast Fourier transform algorithm (Hufton and Danner, 1991; Chen and Hsu, 1987; Hsu and Dranoff, 1987). An alternate way of obtaining analytical information on the concentration distribution is to make use of the well-known moment generating property of Laplace transforms (Douglas, 1972). The various moments of the real-time concentration profile can be related to the transform solution by application of the van der Laan's theorem (Ruthven, 1984):

$$\mu_k = \frac{(-1)^k}{C_o} \lim_{s \rightarrow 0} \frac{\partial^k \bar{C}(s)}{\partial s^k} \quad (20)$$

where

$$\mu_k = \frac{\int_0^\infty t^k C(t) dt}{\int_0^\infty C(t) dt} \quad (21)$$

The normalized moments can be used to calculate central moments, which are often more meaningful in characterizing a distribution (Pawlisch et al., 1987):

$$\mu_k^* = \frac{\int_0^\infty (t - \mu_1)^k C(t) dt}{\int_0^\infty C(t) dt} \quad (22)$$

Application of Eq. 20 to the transform solution, Eq. 18, yields the following pair of moment equations:

$$\mu_1 = \frac{L}{v} \left( 1 + \frac{\epsilon_p}{\epsilon_g} K \right) \quad (23)$$

and

$$L \frac{\mu_2^*}{\mu_1^2} = \frac{2D_L}{v} + \frac{2}{3} \frac{k}{(1+k)^2} \frac{d_f^2}{D_p} v + \frac{2}{3} \frac{k}{(1+k)^2} \frac{KR_p}{k_f} \left( \frac{R_p^3 - R_s^3}{R_p^3} \right) v \quad (24)$$

where  $\mu_1$  is the first temporal moment or mean residence time,  $\mu_2^*$  is the second central moment or variance of the concentration distribution, and  $k$  is the capacity ratio defined as:

$$k = K \frac{\epsilon_p}{\epsilon_g} \quad (25)$$

The lefthand side of Eq. 24 is referred to as the height-equivalent to a theoretical plate (HETP) (Conder and Young, 1979). Each summation on the righthand side of Eq. 24 represents a contribution to peak spreading: axial dispersion in the gas phase, resistance to mass transfer in the polymer phase, and external fluid film resistance. If there are no support particles in the column ( $R_s \rightarrow 0$ ), Eq. 24 becomes:

$$L \frac{\mu_2^*}{\mu_1^2} = \frac{2D_L}{v} + \frac{1}{30} \frac{k}{(1+k)^2} \frac{d_p^2}{D_p} v + \frac{1}{18} \frac{k}{(1+k)^2} \frac{Kd_p^2}{k_f} v \quad (26)$$

The same equation could be derived from the kinetic model proposed by Lee et al. (1988) for a long packed column where intraparticle diffusion with external film resistance occurs.

The longitudinal diffusion coefficient,  $D_L$ , can be approximated as  $D_L = \tau D_m + \lambda v d_p$  (van Deemter et al., 1956), where  $\tau$  is the tortuosity factor which takes into account the irregular pattern along the particles,  $D_m$  is the molecular diffusion coefficient,  $\lambda$  is a packing characterization factor, and  $d_p$  is the particle diameter. Incorporating this approximation into Eq. 24 gives:

$$L \frac{\mu_2^*}{\mu_1^2} = 2\lambda d_p + \frac{2\tau D_m}{v} + \frac{2}{3} \frac{k}{(1+k)^2} \frac{d_p^2}{D_p} v + \frac{2}{3} \frac{k}{(1+k)^2} \frac{KR_p}{k_f} \left( \frac{R_p^3 - R_s^3}{R_p^3} \right) v \quad (27)$$

This equation is very similar to that proposed by van Deemter et al. (1956). In the latter approach, however, analysis of chromatographic data is restricted to Gaussian or symmetric peaks. The use of Eq. 27, on the other hand, along with the statistical moments defined in Eqs. 21–22, extends the model to asymmetric peaks as well.

### Corrections for gas compressibility

In packed-column inverse gas chromatography (PCIGC), the mobile phase expands as it moves through the packed column and encounters lower pressures. This results in a continuous increase in linear velocity through the column. It also results in a continuous increase in the molecular diffusivity in the gas phase. The effect of these variations was elucidated by Giddings et al. (1960) and confirmed by Hawkes (1983). Inclusion of the pressure correction factors into Eq. 27 yields:

$$L \frac{\mu_2^*}{\mu_1^2} = 2\lambda d_p f + \frac{2\tau D_{mo}}{v} j f + \frac{2}{3} \frac{k}{(1+k)^2} \frac{d_p^2}{D_p} v + \frac{2}{3} \frac{k}{(1+k)^2} \frac{KR_p}{k_{fo} j} \left( \frac{R_p^3 - R_s^3}{R_p^3} \right) f v \quad (28)$$

where  $f$  is the compressibility factor of Giddings et al. (1960):

$$f = \frac{9}{8} \frac{[(P_i/P_o)^4 - 1][(P_i/P_o)^2 - 1]}{[(P_i/P_o)^3 - 1]^2} \quad (29)$$

and  $j$  is the James-Martin compressibility factor (Purnell, 1962):

$$j = \frac{3}{2} \frac{[(P_i/P_o)^2 - 1]}{[(P_i/P_o)^3 - 1]} \quad (30)$$

where  $P_i$  and  $P_o$  are the inlet and outlet pressures, respectively. As  $P_i/P_o$  approaches unity,  $f$  and  $j$  approach unity; as  $P_i/P_o$  approaches infinity,  $f$  approaches 9/8 whereas  $j$  approaches zero. In Eq. 28,  $D_{mo}$  and  $k_{fo}$  are the values of  $D_m$  and  $k_f$  evaluated at the outlet pressure,  $P_o$ .

### Evaluation of Model Parameters

Methods of obtaining parameter estimates for the Laplace transform given by Eq. 18 (transfer function) from system response experiments (elution curves) fall into one of four categories: time-domain fitting, method of moments, Laplace domain fitting, and Fourier domain fitting. The merits of each method for IGC applications are discussed by Pawlisch (1985). The analysis has been confined to the use of the method of moments. The Fourier domain fitting method, on the other hand, has been shown to yield more reliable results than the moment fitting method for systems that exhibit low diffusivity in the stationary phase and thus create skewed elution curves with significant tailing (Pawlisch et al., 1988).

### Moment fitting procedures

The equations for the moment-fitting procedure are given in the previous section. The first and second central moments of the elution curves are first obtained by numerical integration of the data according to Eqs. 21 and 22, respectively. These values are usually obtained at different carrier gas flow rates, keeping the other experimental parameters constant (such as temperature and polymer film thickness). The flow rate dependence of the moment data can then be checked for consistency with the model equations. From the first moment values at different carrier gas flow rates, the partition coefficient,  $K$ , is obtained by linear regression of the first moment vs. the retention time of the marker gas,  $t_m$ , which is also the residence time of the carrier gas,  $L/v$ . The ratio  $\epsilon_p/\epsilon_g$  in Eq. 23 is obtained as follows:

$$\frac{\epsilon_p}{\epsilon_g} = \frac{W_p/\rho_p}{F t_m j} \quad (31)$$

Here,  $W_p$  is the weight of the polymer in the column usually determined by soxhlet extraction,  $\rho_p$  is the polymer density at the operating temperature, and  $F$  is the flow rate at the column temperature and outlet pressure. The value of  $K$  is used in the HETP equation (Eq. 28) to estimate the rest of the model parameters:  $D_m$ ,  $D_p$ , and  $k_f$ . Equation 28 may be written in the following manner:

$$L \frac{\mu_2^*}{\mu_1^2} = A f + \frac{B_d j f}{v} + C_p v + C_{so} v \frac{f}{j} \quad (32)$$

where  $A$ , commonly known as the multipath factor, is  $2\lambda d_p$ ,

$B_o$  is the longitudinal diffusion term ( $2\tau D_{mo}$ ), and  $C_p$  is the resistance to mass transfer in the polymer phase:

$$C_p = \frac{2}{3} \frac{k}{(1+k)^2} \frac{d_f^2}{D_p} \quad (33)$$

and  $C_{go}$  is the resistance to mass transfer in the gas phase:

$$C_{go} = \frac{2}{3} \frac{k}{(1+k)^2} \frac{KR_p}{k_{fo}} \left( \frac{R_p^3 - R_s^3}{R_p^3} \right) \quad (34)$$

Assuming a value of  $\tau = 1$ ,  $B_o$  is readily determined since  $D_{mo}$  can be obtained from the Fuller, Schettler and Giddings equation (Reid et al., 1986):

$$D_{mo} = \frac{0.00143 T^{1.75}}{P_o (1/M_A + 1/M_B)^{1/2} [V_A^{1/3} + V_B^{1/3}]^2} \quad (35)$$

where  $M_A$  and  $M_B$  are the molecular weights of the solute and helium, respectively, and  $V_i$  is the special diffusion volume for molecule  $i$ . Purnell (1962) reported values of  $\tau$  ranging from 0.6 to 1. As shown in the section on tests of the PCIGC model, however, the variation of  $\tau$  between 0.6 and 1 has no significant influence on the results. Thus, the imposition of  $\tau$  equal to 1 in the model is not expected to have any deleterious effects. The value of  $A$ , though relatively small in amplitude, can be obtained by regressing its value from high velocity data where Eq. 32 simplifies to:

$$L \frac{\mu_2^*}{\mu_1^2} = Af + cv \quad (36)$$

Here,  $c$  is the overall resistance to mass transfer.

The results for  $A$  and  $B_o$  so determined are then employed to resolve the liquid and gas-phase mass-transfer contributions  $C_p$  and  $C_{go}$ , respectively. A simple mathematical manipulation of Eq. 32 gives:

$$\left( L \frac{\mu_2^*}{\mu_1^2} \frac{j}{f} - Aj - \frac{B_o}{v} j^2 \right) / v = C_p \frac{j}{f} + C_{go} \quad (37)$$

Using the second central moment and the first moment values obtained at different carrier gas velocities  $v$ , and the inlet and outlet pressure values at each velocity to determine  $j$  and  $f$  according to Eqs. 29 and 30, respectively, a plot of the lefthand side of Eq. 37 vs.  $j/f$  should yield a straight line with a slope  $C_p$  and an intercept  $C_{go}$ . The diffusion coefficient of the solute in the polymer phase,  $D_p$ , is then obtained from  $C_p$ , and the mass-transfer coefficient at the outlet pressure,  $k_{fo}$ , is determined from  $C_{go}$ .

### Evaluation of the polymer film thickness

If one assumes that the particles are coated with a uniform polymer film,  $d_f$  can be expressed as follows:

$$d_f = \frac{x}{S_{sp} \rho_p (1-x)} \quad (38)$$

where  $x$  is the percent loading and  $S_{sp}$  is the specific surface

area of the support. The surface area of Chromosorb W-HP was determined through the same procedure adopted by Galin and Rupprecht (1978) and Braun and Guillet (1975). The principle behind this procedure is that for a system consisting of a glassy polymer and a nonsolvent, the retention mechanism is restricted to surface adsorption. In this work,  $n$ -decane, a nonsolvent for polystyrene, was used to obtain the retention volume at several temperatures below the glass transition of polystyrene (that is, 373 K). An average value of 0.185 m<sup>2</sup>/g was obtained for  $S_{sp}$ , in good agreement with the values obtained by Galin and Rupprecht (1978) for two different probes,  $n$ -decane and  $n$ -hexadecane. The specific surface area so determined in this work corresponds to coverage by polystyrene molecules and is referred to as the specific surface area of Chromosorb W-HP accessible to polystyrene.

### Effect of film nonuniformity on model parameters

The presence of film irregularities in a packed column is certainly an unavoidable issue by virtue of the porous character of most chromatographic supports such as Chromosorb W-HP. Such irregularities, however, should not affect the mean retention time of the sample (first moment), as this value depends only on thermodynamic properties and not on the specific geometry of the coating. The second moment or the peak variance, on the other hand, depends on the particular film distribution in the column. The effect of film irregularities can be evaluated more easily in the case of capillary columns. Pawlisch (1985) and Hadj Romdhane et al. (1992) have examined this case and reported that for the maximum variation in the film thickness between a uniform coating and a highly nonuniform coating, the diffusion coefficient varies only by a factor of 2. Thus, one can speculate that the effect of film nonuniformity in the packed column could also lead to diffusivity variations of a factor of 2. In the packed column, however, the film is on average distributed in a fashion somewhere between the uniform and highly nonuniform cases considered in the capillary column. It was therefore concluded that the apparent or measured diffusivity in a packed column based on a uniform film assumption should be very close to the true diffusivity. As shown in the results section, this conclusion is borne out by the experimental data.

### Experimental Studies

Measurements were carried out on a Varian 3400 gas chromatograph, equipped with an autosampler and a thermal conductivity detector. Helium was used as the carrier gas in all experiments. The temperature of the injection block and the detector assembly were set about 50°C above the column temperature to avoid condensation in the detector assembly. Small amounts of solvent (<0.1  $\mu$ L) were injected through the rubber septum of the injection port into the carrier gas using a Hamilton 1- $\mu$ L syringe. Usually, about 0.8  $\mu$ L of air was injected along with the liquid sample as the inert component to determine the average velocity of the carrier gas in the column. Retention time data were found to be independent of solute sample size. The output from the thermal conductivity detector was fed to the printer/plotter built into the gas chromatograph and to a data system (DS-654) for further analysis of the chromatographic peaks.

The carrier gas flow rate was measured by means of a soap bubble flowmeter. To eliminate any uncertainty caused by partial saturation from the soap solution in the bubble flowmeter, the carrier gas was saturated with water immediately after passing through the detector. At each temperature, measurements were made over a wide range of flow rates ranging from 20 to 110 cm<sup>3</sup>/min. In addition, replicate experiments were done at each flow rate to insure that the results were reproducible at a fixed set of conditions. After each flow rate study, the pressure drop across the column was measured by means of a pressure transducer and the column set to the next flow rate.

Two chromatographic columns (columns A and B) were used throughout this study. Both columns were 1/8-in. (3.2-mm)-OD, 6-ft (152-m)-long stainless steel tubing, packed with Chromosorb W-HP (80–100 mesh) support which was coated with monodisperse polystyrene ( $M_n=68,700$ ). The percent loading of the coated material packed in columns A and B was determined by soxhlet extraction to be 14.96% and 11.7%, respectively. The corresponding amount and approximate film thickness of polystyrene in each column was 0.2975 g (0.96 micron) in column A and 0.2283 g (0.71 micron) in column B.

## Results and Discussion

### Tests of the PCIGC model

The consistency of the model was checked by testing the flow rate dependence of the moment values obtained from the chromatographic data of the PS-toluene and the PS-benzene systems at temperatures above  $T_{g2}$  using column A. In this test, the first moment and the second central moment were determined either according to Eqs. 21 and 22 or directly from the retention time at the peak maximum and the peak width at half-height, as suggested by Conder and Young (1979):

$$L \frac{\mu_2^*}{\mu_1^2} = \frac{L}{5.54} \left( \frac{w_{1/2}}{t_r} \right)^2 \quad (39)$$

Here,  $w_{1/2}$  is the peak width at half-height and  $t_r$  is the retention time of the solvent obtained at the maximum of the peak. No significant difference was found between these two approaches.

For the implementation of Eqs. 21 and 22, a computer program was written for the data acquisition computer which processed the data from the gas chromatograph. In this program, the raw output signal is corrected for baseline offset since the model assumes that the baseline signal is zero. Then, once a range of integration limits was selected, the program integrated and normalized the data file, and calculated the first and second central moments according to Eqs. 21 and 22.

According to Eq. 23, the first moment,  $\mu_1$ , changes linearly with the retention time of the marker gas,  $t_m$  or  $L/v$ , and depends only on the thermodynamic properties of the polymer-solute system. To verify this behavior, a plot of the first moment vs.  $t_m$  was performed. Figure 1 illustrates the linear behavior of  $\mu_1$  with  $t_m$  for PS-toluene at 413 and 433 K. The partition coefficient values were determined to be 35.5 at 413 K and 23.8 at 433 K, which yield weight-fraction activity coefficient values of 5.17 and 5.23, respectively, in good agreement with other results (Hadj Romdhane and Danner, 1991; New-

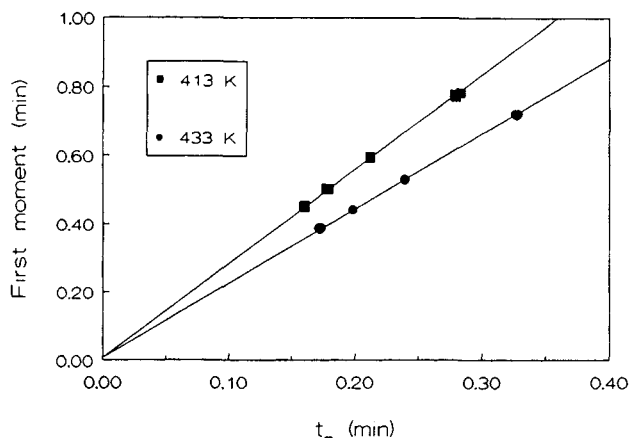


Figure 1. First moment analysis for the PS-toluene system at 413 and 433 K.

man and Praunzitz, 1972; Galin and Rupprecht, 1978). The partition coefficient values obtained at each temperature were then used in Eq. 37 to estimate the diffusion coefficient in the polymer phase,  $D_p$ , and the mass-transfer coefficient,  $k_{fo}$ .

The dependence of the central second moment on flow rate, as suggested by Eq. 37, is typified in Figure 2 for the PS-toluene system at 403, 413 and 433 K. The lefthand side of Eq. 37 is given the symbol  $H_{m2}/v$  in this figure, where  $H_{m2}$  is the plate height arising from only mass-transfer effects. As shown in Figure 2, the data are fit adequately by straight lines in agreement with Eq. 37. Similar agreement was found at other temperatures and for the PS-benzene system as well. The diffusion coefficients generated in this work for toluene and benzene in polystyrene are compiled in Table 1. The  $\tau$  value was set to 1 in all cases, since its variation did not affect the results appreciably. For example, a  $\tau$  value of 0.6 yields a diffusion coefficient value of  $8.25 \times 10^{-9}$  cm<sup>2</sup>/s at 413 K and  $6.31 \times 10^{-8}$  cm<sup>2</sup>/s at 433 K for the PS-toluene system. The differences between these results and those reported in Table 1 are not significant. Thus, a  $\tau$  value of 1 can be used as long as axial dispersion effects are negligible. Finally, the effect of polymer film thickness was checked by determining the diffusion coefficient of toluene in polystyrene at 403 K from the chromatographic data generated with column B. The same data

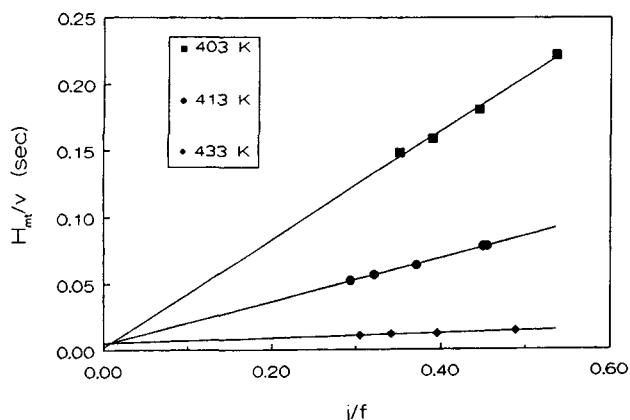


Figure 2. Estimation of  $D_p$  for the PS-toluene system.

**Table 1. Diffusion Coefficients of Toluene and Benzene in PS at Infinite Dilution ( $\text{cm}^2/\text{s} \times 10^9$ )**

Solvent	Column	$T$ (K)	Diffusivity
Toluene	A	403	2.79
Toluene	B	403	1.95
Toluene	A	413	8.61
Toluene	A	413	8.41
Toluene	A	423	28.8
Toluene	A	433	83.3
Toluene	A	433	78.2
Benzene	A	403	3.93
Benzene	A	413	12.6
Benzene	A	423	42.9
Benzene	A	428	64.9
Benzene	A	433	117.0

analysis procedure described above for column A was carried out with column B, and the resulting value for  $D_p$  was  $1.95 \times 10^{-9} \text{ cm}^2/\text{s}$ . This value is again in good agreement with that reported for column A ( $2.79 \times 10^{-9} \text{ cm}^2/\text{s}$ ), indicating that there is no effect of film thickness on the diffusion results.

One disadvantage of the method of moments for parameter estimation, however, is that the procedure is not model-discriminatory; distributions with radically different shapes can have identical first and second moments (Pawlisch et al., 1987). It was therefore necessary to confirm that the parameter estimates from the moment analysis correctly reproduce the original elution curves. Such a comparison is shown in Figure 3 for the elution curve obtained for PS-toluene at 413 K with an average velocity of 11.7 cm/s. In this diagram, the points were taken from the experimental elution curve, while the solid line is the theoretical elution curve (Eq. 18) generated with values of  $K$ ,  $D_L$ ,  $D_p$ , and  $k_f$  obtained from moment measurements. Inversion of the Laplace transform solution was done numerically with a Fast Fourier Transform algorithm. Clearly, the parameters obtained from moment analysis reproduced the original elution curve very well. Comparisons of theoretical and experimental curves for other cases showed similar agreement, which proves that the theoretical model developed in this study accurately describes the chromatographic process.

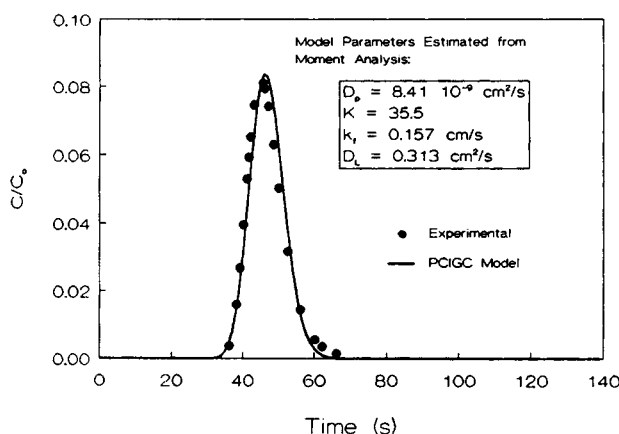


**Figure 3. Comparison of experimental and theoretical elution profiles for the PS-toluene system at 413 K ( $v = 11.67 \text{ cm/s}$ ).**

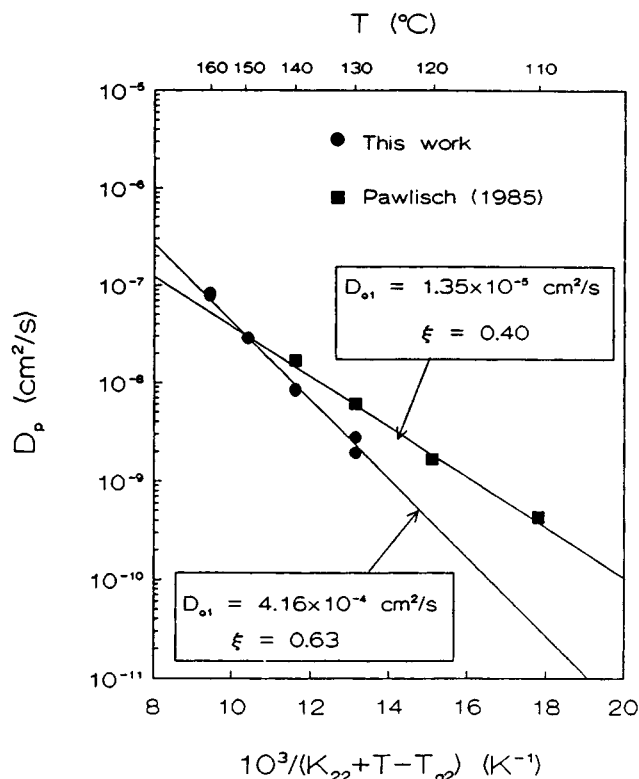


**Figure 4. Free-volume correlation of the diffusivity data of toluene in polystyrene.**

### Tests of the free-volume theory

**Polystyrene-Toluene.** The diffusion coefficients reported in the previous section for the PS-toluene system are plotted in Figure 4 along with the values obtained by Pawlisch (1985). The solid lines connecting each data set represent a correlation of the diffusion coefficient data with temperature according to the free-volume theory which simplifies to the following expression at zero solvent mass fraction:

$$D_p = D_{o1} \exp \left[ \frac{-\gamma \bar{V}_2^* \xi}{K_{12}(K_{22} - T_{g2} + T)} \right] \quad (40)$$

Here,  $\bar{V}_2^*$  is the specific critical hole-free volume of the polymer required for a jump,  $\gamma$  is an overlap factor,  $K_{12}$  and  $K_{21}$  are the free-volume parameters for the polymer,  $T_{g2}$  is the glass transition temperature of the polymer,  $D_{o1}$  is a preexponential factor which is assumed to be independent of temperature, and  $\xi$  is the ratio of the molar volume of the solvent jumping unit to the molar volume of the polymer jumping unit. The parameters,  $D_{o1}$  and  $\xi$  reported for each data set in Figure 4, were determined by linear regression in  $\ln D_p$  vs.  $(K_{22} - T_{g2} + T)^{-1}$ . While the correlations indicate that the temperature dependence of the diffusion coefficients in each study is well captured by the free-volume theory, the scatter between the diffusion coefficients obtained in this work and those reported by Pawlisch (1985) led to a substantial disagreement in the regressed parameters:  $D_{o1}$  and  $\xi$ . To interpret these differences, both sets of data were compared against the diffusivity data collected by Duda et al. (1982) by means of the vapor sorption technique, as shown in Figure 5. Duda et al.

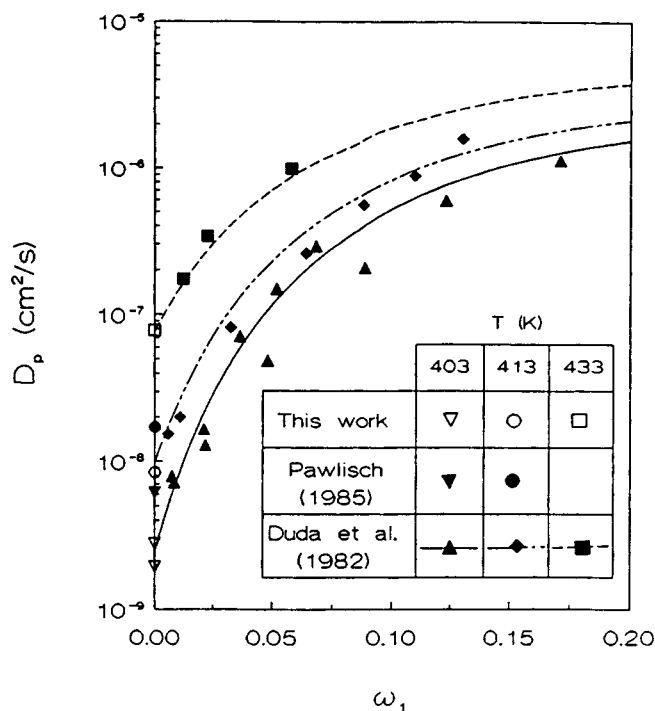


Figure 5. Comparison of IGC and vapor sorption data for the diffusivity of toluene in polystyrene.

correlated their diffusion data using the free-volume theory, and the regressed parameters were used to construct the dashed and solid curves at different temperatures in Figure 5. The values obtained by extrapolation of the vapor sorption data to infinite dilution seem to agree very well with the values obtained in this work, while those reported by Pawlisch (1985) were consistently higher at 403 and 413 K. The good agreement between the diffusion data obtained in this work and the extrapolated vapor sorption diffusion data over the entire temperature range investigated indicates that the current data are more consistent with the vapor sorption measurements than those reported by Pawlisch (1985). The differences between the current diffusivity data and those reported by Pawlisch, however, are not surprising in view of the general difficulty of measuring diffusion data.

**Polystyrene-Benzene.** A similar test of the free-volume theory was made using the diffusivity data reported earlier for the PS-benzene system. Figure 6 is a comparison, in terms of a free-volume correlation, of the values obtained in this work and those reported by Pawlisch (1985). The  $D_{o1}$  and  $\xi$  values shown in Figure 6 were determined for the PS-benzene system as described above. Once again, the results obtained in this work were found to be in disagreement with those of Pawlisch as portrayed by the notable differences in  $D_{o1}$  and  $\xi$ . These two parameters are very important since they significantly affect the concentration and temperature dependence of the mutual and self-diffusion coefficients. The  $D_{o1}$  and  $\xi$  values obtained in this study and those obtained by correlation of the diffusivity data of Pawlisch (1985) were used to describe the concentration dependence of the self-diffusion coefficient of benzene in PS.

The expression for the self-diffusion coefficient as derived by Vrentas and Duda (1977a,b) is:

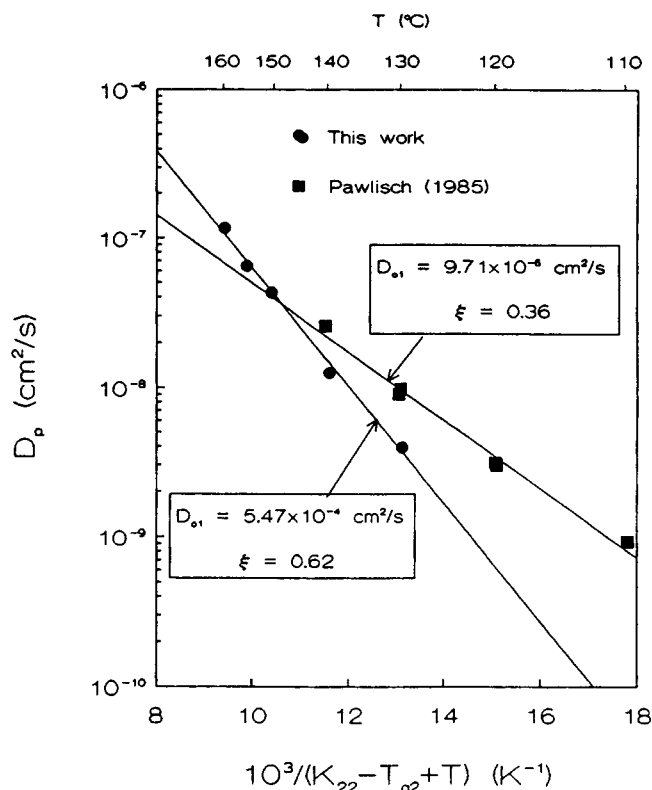


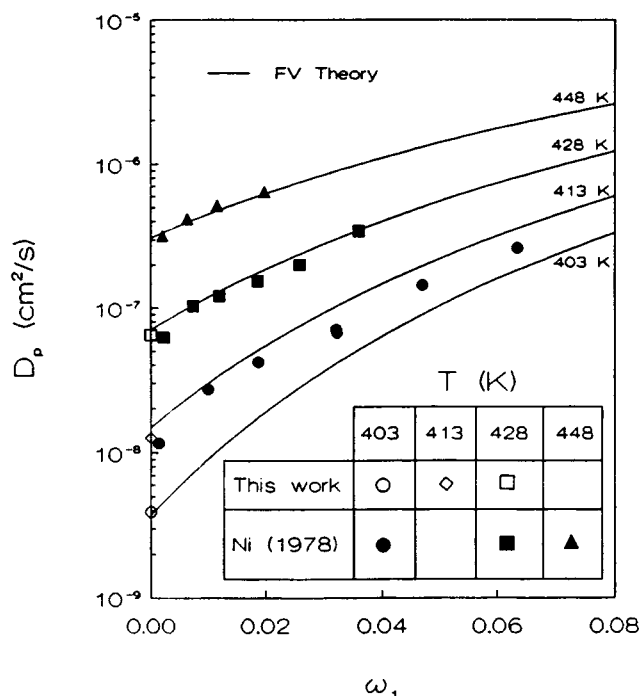
Figure 6. Free-volume correlation of the diffusivity data of benzene in polystyrene.

$$D_1 = D_{o1} \exp \left[ \frac{-(w_1 \bar{V}_1^* + w_2 \xi \bar{V}_2^*)}{w_1 \frac{K_{11}}{\gamma} (K_{21} - T_{g1} + T) + w_2 \frac{K_{12}}{\gamma} (K_{22} - T_{g2} + T)} \right] \quad (41)$$

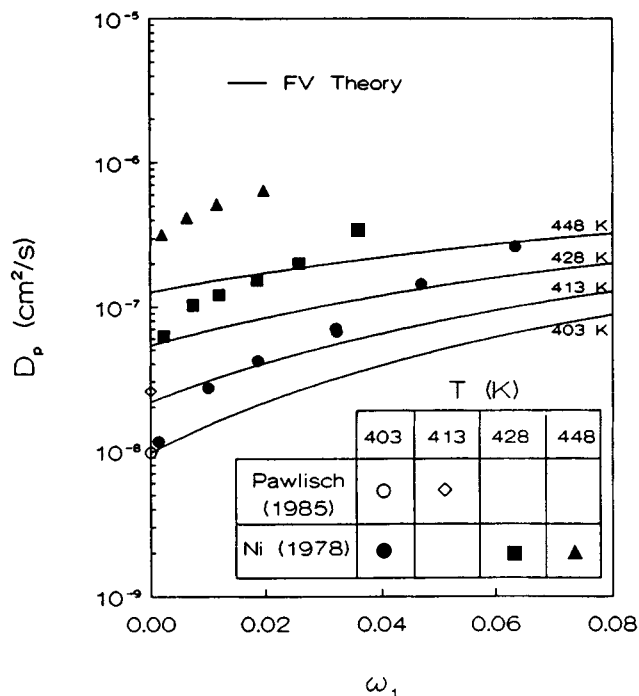
where  $\bar{V}_i^*$  is the specific critical hole-free volume of component  $i$  required for a jump,  $w_i$  is the mass fraction of component  $i$ , and  $K_{11}$  and  $K_{21}$  are the free-volume parameters for the solvent. The two critical volumes,  $\bar{V}_1^*$  and  $\bar{V}_2^*$ , are estimated from the specific volumes of the solvent and polymer at absolute zero temperature, respectively, using group contribution methods developed by Sugden (1927) and Biltz (1934). The free-volume parameters,  $K_{1i}/\gamma$  and  $K_{2i} - T_{gi}$ , for the solvent and the polymer are obtained by correlating pure-component viscosity data with temperature as suggested by Williams et al. (1955). A compilation of these parameters for a large number of solvents and polymers was presented by Zielinski and Duda (1992). The two parameters remaining to be determined in the self-diffusion equation are  $D_{o1}$  and  $\xi$ , which are, as shown above, easily obtained by the inverse gas chromatography method.

Figure 7 shows the results of the free-volume theory predictions for the case where  $D_{o1}$  and  $\xi$  determined in this work were used, as well as a comparison with the vapor sorption data reported by Ni (1978). The agreement is remarkable at 428 K and 448 K, but not as good at 403 K. No explanation for this discrepancy has been found yet. Similarly, Figure 8 illustrates the comparison between the data of Ni and the free-volume theory predictions using the  $D_{o1}$  and  $\xi$  from the data





**Figure 7. Prediction of the self-diffusion coefficient of benzene in polystyrene at low concentrations using the values of  $D_{o1}$  and  $\xi$  obtained in this work.**



**Figure 8. Prediction of the self-diffusion coefficient of benzene in polystyrene at low concentrations using the values of  $D_{o1}$  and  $\xi$  obtained from the data of Pawlich (1985).**

of Pawlich (1985). Though the diffusion data point obtained by Pawlich at 403 K seems to be in good agreement with the extrapolated vapor sorption data, the predictions at this temperature as well as at all the other temperatures considered, follow a completely different trend with concentration than that observed experimentally. To examine further the effects of the differences in the  $D_{o1}$  and  $\xi$  values of Pawlich and the current work, the predictions obtained were compared against the PS-benzene diffusivity values reported by Kosfeld and Zunkley (1979) which were obtained at temperatures and concentrations far outside the range of this study by means of the spin-echo nuclear magnetic resonance (NMR) technique. The comparisons are shown in Figure 9. The symbols represent the NMR self-diffusion coefficient data at different temperatures, the solid curves are the free-volume theory predictions based on the values of  $D_{o1}$  and  $\xi$  from this work, and the dashed curves are the free-volume theory predictions based on the values of  $D_{o1}$  and  $\xi$  correlated from the data of Pawlich (1985). Clearly, the agreement between the experimental data and the current data is superior to that illustrated between experimental data and the data of Pawlich. The results shown in Figures 7, 8 and 9 suggest that the current data are more consistent with both the vapor sorption measurements and the NMR measurements.

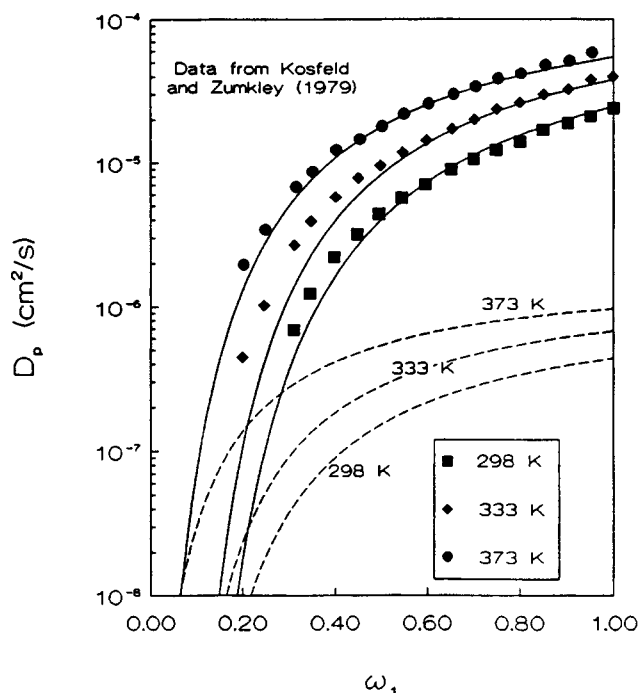


**Figure 9. Prediction of the self-diffusion coefficient of benzene in polystyrene at high concentrations.**

—, free-volume predictions based on the  $D_{o1}$  and  $\xi$  values obtained in this work; ---, free-volume predictions based on the  $D_{o1}$  and  $\xi$  values obtained from the data of Pawlich (1985).

## Conclusions

A mathematical model describing the elution process in packed columns where the stationary phase is a polymeric material was developed. The first and second central moments derived from this model relate the elution characteristics of the peak (residence time and shape of the elution curve) to the

thermodynamic and transport properties of the polymer-solvent system. The validity of the moment analysis model was demonstrated by measuring the solubility and diffusivity of benzene and toluene in polystyrene at temperatures above  $T_{g2}$ . The diffusivity data collected in this work by packed-column IGC were compared against previous results obtained by means of three other different techniques: capillary-column IGC (Pawlisch, 1985), vapor sorption (Duda et al., 1982; Ni, 1978), and echo-spin NMR (Kosfeld and Zumkley, 1979). Some systematic differences were found between the current diffusion data and those reported by Pawlisch. The current data were shown to be highly consistent with the previous vapor sorption and NMR measurements. It has been demonstrated that one can use the results obtained at infinite dilution to predict reliably via the free-volume theory the concentration and temperature dependence of the PS-benzene diffusion coefficients. Packed-column inverse gas chromatography thus proves to be a convenient tool for the study of mass-transfer kinetics, provided that a correct mathematical interpretation of the elution process is used.

## Acknowledgment

Financial support of this research by the 3M company, St. Paul, MN, is gratefully acknowledged. The authors thank Professor J. L. Duda for his advice throughout this work, as well as Dr. J. R. Hufton and Dr. J. M. Zielinski for helpful discussions on theoretical and experimental aspects of this study.

## Notation

- $A$  = multipath factor, cm
- $B_o$  = axial dispersion term,  $\text{cm}^2/\text{s}$
- $c$  = overall resistance to mass transfer, s
- $C$  = solute concentration in the gas phase,  $\text{mol}/\text{cm}^3$
- $C_o$  = strength of the inlet impulse
- $C_{go}$  = resistance to mass transfer in the gas phase, s
- $C_p$  = resistance to mass transfer in the polymer phase, s
- $D_{ol}$  = constant preexponential factor,  $\text{cm}^2/\text{s}$
- $d_f$  = polymer film thickness, cm
- $D_L$  = longitudinal diffusion coefficient,  $\text{cm}^2/\text{s}$
- $D_m$  = solute diffusion coefficient in the mobile phase,  $\text{cm}^2/\text{s}$
- $d_p$  = particle diameter, cm
- $D_p$  = solute diffusion coefficient in the polymer phase,  $\text{cm}^2/\text{s}$
- $f$  = Giddings compressibility factor
- $F$  = flow rate at column temperature and outlet pressure,  $\text{cm}^3/\text{s}$
- $j$  = James-Martin compressibility factor
- $k$  = capacity ratio defined by Eq. 25
- $K$  = equilibrium partition coefficient of the polymer-solvent system
- $K_{i1}$  = free-volume parameter of component  $i$ ,  $\text{cm}^3/\text{g} \cdot \text{K}$
- $K_{2i}$  = free-volume parameter of component  $i$ , K
- $k_f$  = fluid film mass-transfer coefficient,  $\text{cm}/\text{s}$
- $L$  = length of the column, cm
- $M_i$  = molecular weight of component  $i$ , g/mol
- $Pe$  = Peclet number defined by Eq. 19
- $P_i$  = column inlet pressure, atm
- $P_o$  = column outlet pressure, atm
- $q$  = solute concentration in the polymer phase,  $\text{mol}/\text{cm}^3$
- $Q$  = volume-average concentration of solute in the polymer phase,  $\text{mol}/\text{cm}^3$
- $r$  = radial coordinate, cm
- $R_p$  = radius of the polymer film, cm
- $R_s$  = radius of the support particle, cm
- $S_{sp}$  = specific surface area of the support,  $\text{cm}^2/\text{g}$
- $t$  = time, s
- $T$  = column temperature, K
- $T_{gi}$  = glass-transition temperature of component  $i$ , K
- $t_m$  = retention time of air, s
- $t_r$  = solute retention time at the peak maximum, s

- $v$  = average linear velocity of the carrier gas,  $\text{cm}/\text{s}$
- $V_i$  = diffusion volume of molecule  $i$ ,  $\text{cm}^3/\text{mol}$
- $\bar{V}_i^*$  = specific critical hole free-volume of component  $i$ ,  $\text{cm}^3/\text{g}$
- $w_{1/2}$  = width of the peak at half-height, s
- $w_i$  = mass fraction of component  $i$
- $W_p$  = weight of polymer in the column, g
- $x$  = percent loading
- $z$  = axial coordinate, cm

## Greek letters

- $\gamma$  = overlap factor to account for shared free volume
- $\delta(t)$  = Dirac delta function
- $\epsilon_p$  = fractional volume of the stationary phase
- $\epsilon_g$  = fractional volume of the mobile phase
- $\lambda$  = packing characterization factor
- $\mu_1$  = first temporal moment, s
- $\mu_2$  = variance of the concentration distribution,  $\text{s}^2$
- $\mu_k$  =  $k$ th normalized moment of the elution curve
- $\mu_k$  =  $k$ th central moment of the elution curve
- $\xi$  = ratio of solvent and polymer jumping units
- $\rho_p$  = polymer density at column temperature,  $\text{g}/\text{cm}^3$
- $\tau$  = obstruction factor

## Literature Cited

- Arnould, D., and R. L. Laurence, "Inverse Gas Chromatography," *ACS Symp. Ser.*, No. 391, D. R. Lloyd, T. C. Ward, H. P. Shreiber, eds., Washington, DC, 87 (1989).
- Biltz, W., *Rauchemie der Festen Stoffe*, Voss, Leipzig (1934).
- Braun, J.-M., and J. E. Guillet, "Studies of Polystyrene in the Region of the Glass Transition Temperature by Inverse Gas Chromatography," *Macromol.*, **8**, 882 (1975).
- Chen, T.-L., and J. T. Hsu, "Prediction of Breakthrough Curves by the Application of Fast Fourier Transform," *AIChE J.*, **33**, 1387 (1987).
- Conder, J. R., and C. L. Young, *Physicochemical Measurement by Gas Chromatography*, Wiley, New York (1979).
- Douglas, J. M., *Process Dynamics and Control: Analysis of Dynamic Systems*, Prentice Hall, Englewood Cliffs, NJ (1972).
- Duda, J. L., J. S. Vrentas, S. T. Ju, and H. T. Liu, "Prediction of Diffusion Coefficients for Polymer-Solvent Systems," *AIChE J.*, **28**, 279 (1982).
- Galin, M., and M. C. Rupprecht, "Study by Gas-Liquid Chromatography of the Interactions Between Linear or Branched Polystyrenes and Solvents in the Temperature Range 60°–200°C," *Polymer*, **19**, 506 (1978).
- Giddings, J. C., S. L. Seager, L. R. Stucki, and G. H. Stewart, "Plate Height in Gas Chromatography," *Anal. Chem.*, **32**, 867 (1960).
- Gray, D. G., and J. E. Guillet, "Studies of Diffusion in Polymers by Gas Chromatography," *Macromol.*, **6**, 223 (1973).
- Hadj Romdhane, I., and R. P. Danner, "Solvent Volatilities from Polymer Solutions by Gas-Liquid Chromatography," *J. Chem. Eng. Data*, **36**, 15 (1991).
- Hadj Romdhane, I., R. P. Danner, and J. L. Duda, "Solute Diffusion in Polymers by Inverse Gas-Liquid Chromatography," *AIChE Meeting*, Miami Beach, FL (Nov., 1992).
- Hawkes, S. J., "Modernization of the van Deemter Equation for Chromatographic Zone Dispersion," *J. Chem. Educ.*, **60**, 393 (1983).
- Hsu, J. T., and J. S. Dranoff, "Numerical Inversion of Certain Laplace Transforms by the Direct Application of Fast Fourier Transform (FFT) Algorithm," *Comput. Chem. Eng.*, **11**, 101 (1987).
- Hu, D. S., C. D. Han, and L. I. Stiel, "Gas Chromatographic Measurements of Infinite Dilution Diffusion Coefficients of Volatile Liquids in Amorphous Polymers at Elevated Temperatures," *J. Appl. Polym. Sci.*, **33**, 551 (1987).
- Hufton, J. R., and R. P. Danner, "Gas-Solid Diffusion and Equilibrium Parameters by Tracer Pulse Chromatography," *Chem. Eng. Sci.*, **46**, 2079 (1991).
- Kong, J. M., and S. J. Hawkes, "Diffusion in Silicone Stationary Phases," *J. Chromatog. Sci.*, **14**, 279 (1976).
- Kosfeld, R., and L. Zumkley, "Mobility of Small Molecules in Polymer Systems," *Ber. Bunsenges. Phys. Chem.*, **83**, 392 (1979).

- Lee, W.-C., S. H. Huang, and G. T. Tsao, "A Unified Approach for Moments in Chromatography," *AIChE J.*, **34**, 2083 (1988).
- Newman, R. D., and J. M. Prausnitz, "Polymer-Solvent Interactions from Gas-Liquid Partition Chromatography," *J. Phys. Chem.*, **76**, 1492 (1972).
- Ni, Y. C., "Evaluation of Free Volume Theory for Molecular Diffusion in Polymer Solutions," PhD thesis, Pennsylvania State Univ., University Park (1978).
- Pawlisch, G. A., "Measurement of the Diffusivity and Thermodynamic Interactions Parameters of a Solute in a Polymer Melt Using Capillary Column Inverse Gas Chromatography," PhD thesis, Univ. of Massachusetts (1985).
- Pawlisch, G. A., A. Macris, and R. L. Laurence, "Solute Diffusion in Polymers: 1. The Use of Capillary Column Inverse Gas Chromatography," *Macromol.*, **21**, 1564 (1987).
- Pawlisch, G. A., J. R. Bric, and R. L. Laurence, "Solute Diffusion in Polymers: 2. Fourier Estimation of Capillary Column Inverse Gas Chromatographic Data," *Macromol.*, **20**, 1685 (1988).
- Purnell, J. H., *Gas Chromatography*, Wiley, New York (1962).
- Ruthven, D. M., *Principles of Adsorption and Adsorption Processes*, Wiley, New York (1984).
- Reid, R. C., J. M. Prausnitz, and B. E. Poling, *The Properties of Gases and Liquids*, 4th ed., McGraw-Hill, New York (1986).
- Sugden, S., "Molecular Volumes at Absolute Zero: II. Zero Volumes and Chemical Composition," *J. Chem. Soc.*, 1786 (1927).
- Tait, G. T., and A. M. Abushihada, "The Use of a Gas Chromatographic Technique for the Study of Diffusion in Polymers," *J. Chromatog. Sci.*, **17**, 219 (1979).
- van Deemter, J. J., F. J. Zuiderweg, and A. Klinkenberg, "Longitudinal Diffusion and Resistance to Mass Transfer as Causes of Nonideality in Chromatography," *Chem. Eng. Sci.*, **5**, 271 (1956).
- Vrentas, J. S., and J. L. Duda, "Diffusion in Polymer-Solvent Systems: I. Reexamination of the Free-Volume Theory," *J. Poly. Sci: Part B: Poly. Phys.*, **15**, 403 (1977a).
- Vrentas, J. S., and J. L. Duda, "Diffusion in Polymer-Solvent Systems: II. A Predictive Theory for the Dependence of Diffusion Coefficients on Temperature, Concentration, and Molecular Weight," *J. Poly. Sci: Part B: Poly. Phys.*, **15**, 417 (1977b).
- Williams, M. L., R. F. Landel, and J. D. Ferry, "The Temperature Dependence of Relaxation Mechanisms in Amorphous Polymers and Other Glass-Forming Liquids," *J. Amer. Chem. Soc.*, **77**, 3701 (1955).
- Zielinski, J. M., and J. L. Duda, "Predicting Polymer/Solvent Diffusion Coefficients Using Free-Volume Theory," *AIChE J.*, **38**, 405 (1992).

Manuscript received June 8, 1992, and revision received Jan. 19, 1993.